

Supporting Information

Undifferentiated Destruction of Mitochondria by Photoacoustic Shockwave to Overcome Chemo and Radiation Resistance in Cancer Therapy

Liming Liu,^{a, b} Fanchu Zeng,^{a, b} Yujie Li,^c Wenjing Li,^{a, b} Hui Yu,^d Qingxing Zeng,^d Qun Chen,^{*a, b}

Huan Qin^{*a, b, c}

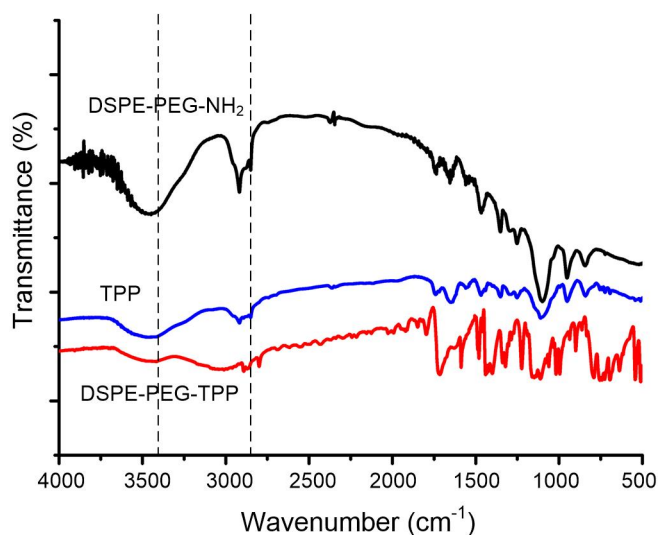


Figure S1: The FT-IR spectrum of DSPE-PEG-NH₂, TPP, DSPE-PEG-TTP.

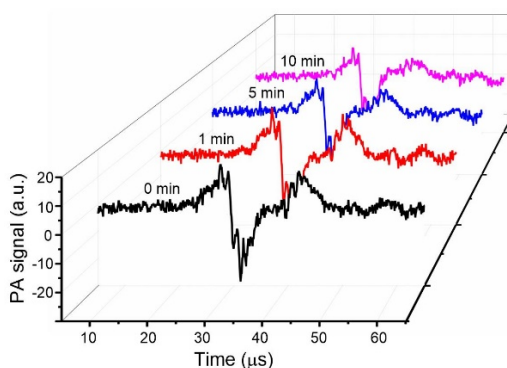


Figure S2. Photoacoustic signal generated from the ICG/DSPE-PEG-TTP in different time.

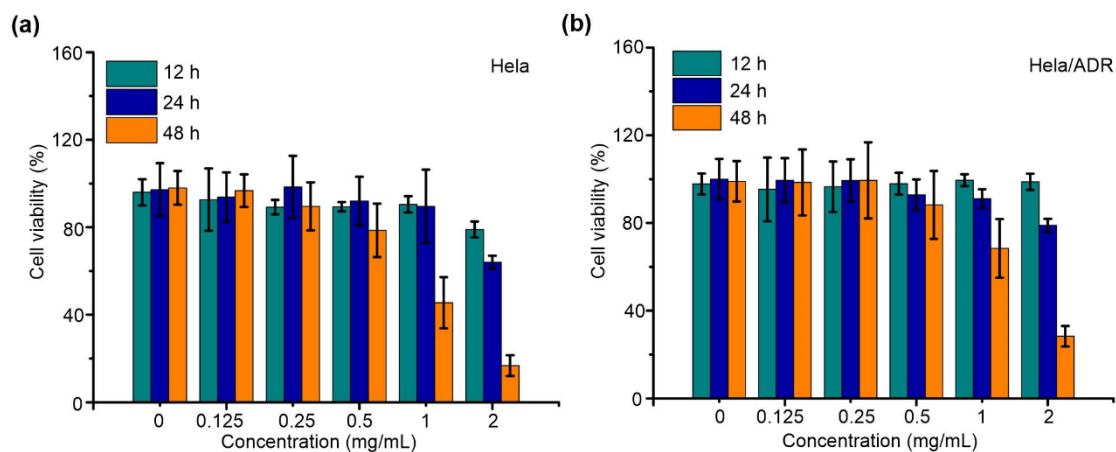


Figure S3. The cellular co-incubation with ICG/DSPE-PEG-TPP at different time points and different concentrations. The experiment was examined against (a) HeLa and (b) HeLa/ADR cells by CCK-8 assay at 12 h, 24 h, 48 h with different concentrations from 0 to 2 mg mL⁻¹

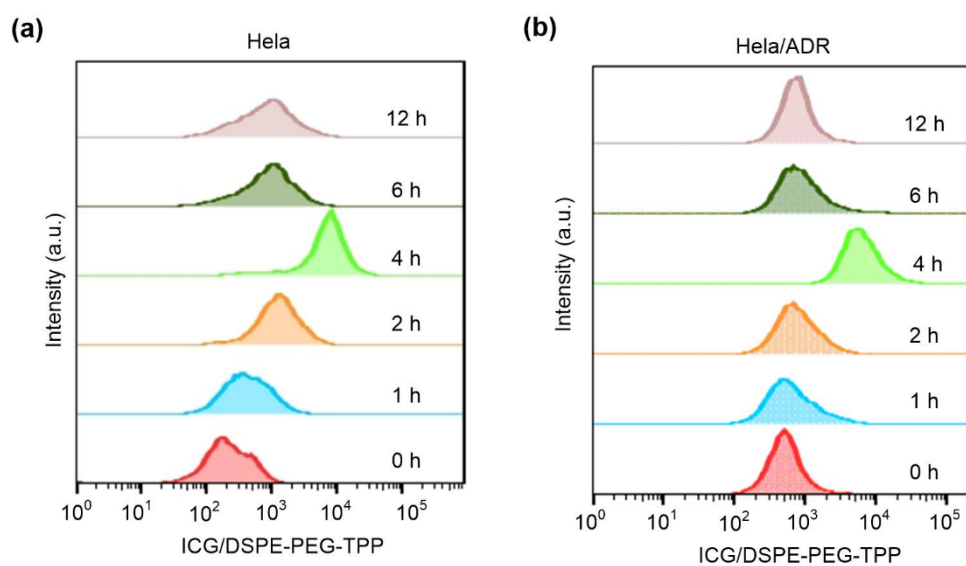


Figure S4. The cellular uptake of ICG/DSPE-PEG-TPP at different time points. The cellular uptake of ICG/DSPE-PEG-TPP (1 mg mL⁻¹) was examined against (a) HeLa and (b) HeLa/ADR cells by FACS at 0 h, 1 h, 2 h, 4 h, 6 h, 12 h.

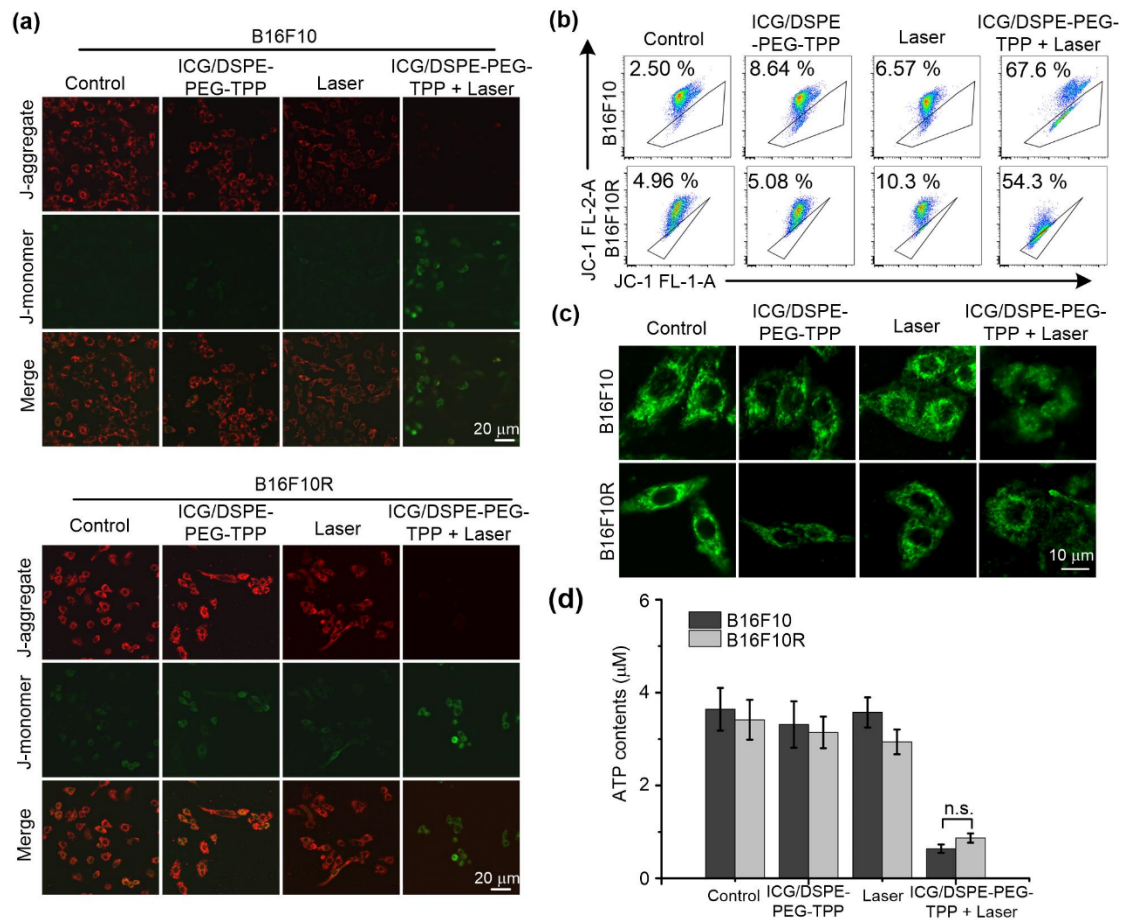


Figure S5. To examine the effect of PA shockwave on mitochondria of the tumor cells. (a) CLSM images of B16F10 and B16F10R cells stained with JC-1 after different treatments, the fluorescence transition from red to green indicated significant mitochondrial damage. (scale bar, 20 μm). (b) FACS analysis of B16F10 and B16F10R stained with JC-1 under different treatments. (c) CLSM imaging of mitochondrial morphology in B16F10 and B16F10R cells after different treatments, the cells were stained with MitoTracker green. (scale bar, 10 μm). (d) B16F10 and B16F10R cells were treated with different treatments for the cellular ATP measurement. Data are shown as mean \pm SD (n = 3). * $p < 0.05$, ** $p < 0.01$, *** $p < 0.001$.

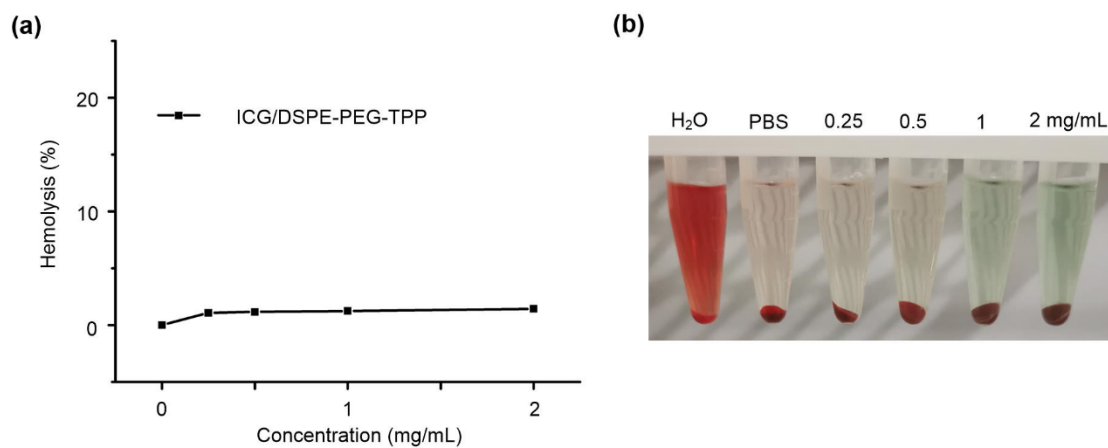


Figure S6. Toxicity evaluation of ICG/DSPE-PEG-TPP via hemolysis test. Hemolysis ratio of ICG/DSPE-PEG-TPP with different concentrations from 0 to 2 mg mL⁻¹.

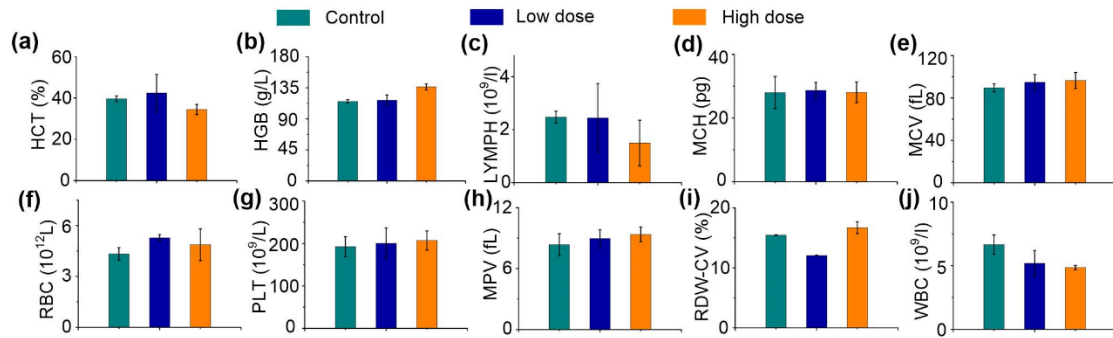


Figure S7. *In vivo* biocompatibility of mice 7 days after injection of ICG/DSPE-PEG-TPP at two different doses. Haematological data of the mice intravenously injected with different dose of ICG/DSPE-PEG-TPP at the 7 days post-injection. The terms are noted as followed: (a) haematocrit (HCT), (b) haemoglobin (HGB), (c) Lymphocyte number (LYMPH), (d) mean corpuscular haemoglobin (MCH), (e) mean corpuscular volume (MCV), (f) red blood cells (RBC), (g) platelets (PLT), (h) mean platelet volume (MPV), (i) coefficient of red cell width distribution (RDW-CV) and (j) white blood cells (WBC), (Low dose: 5 mg kg⁻¹, High dose: 50 mg kg⁻¹, 100 μL, n = 3).

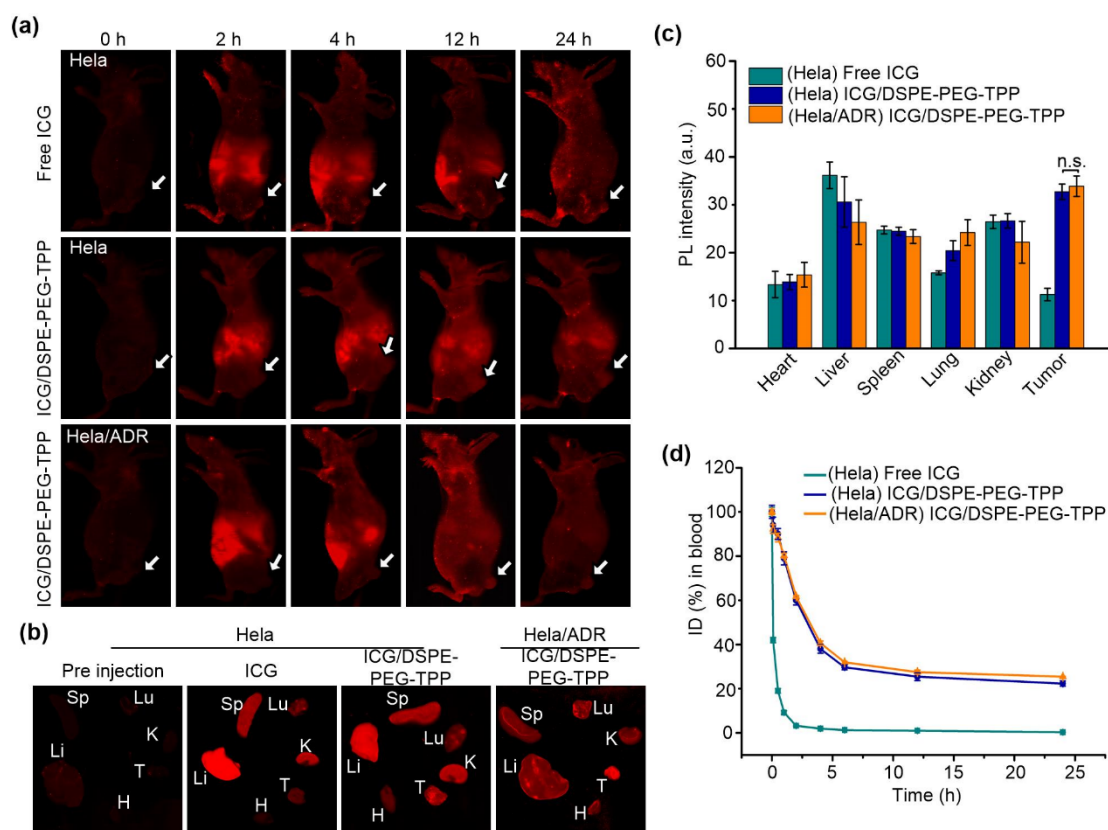


Figure S8. *In vivo* pharmacodynamics evaluation of ICG/DSPE-PEG-TPP. (a) *In vivo* fluorescent imaging of HeLa, HeLa/ADR tumor bearing mice upon treatment with free ICG and ICG/DSPE-PEG-TPP at 0 h, 2 h, 4 h, 12 h, 24 h. (b) The main organs and tumor tissues were spectrally imaged by the ODYSSEY Infrared Imaging System. Typical fluorescent images and (c) quantification of major organs and tumors collected from mice treated with free ICG and ICG/DSPE-PEG-TPP after 24 h post-injection ($p = 0.451$, *n.s.*: no significance). (d) Blood circulation profiles of ICG/DSPE-PEG-TPP and free ICG. (Lu: Lung, Li: Liver, Sp: Spleen, H: Heart, T: Tumor, K: Kidney). Data are shown as mean \pm SD ($n = 3$).

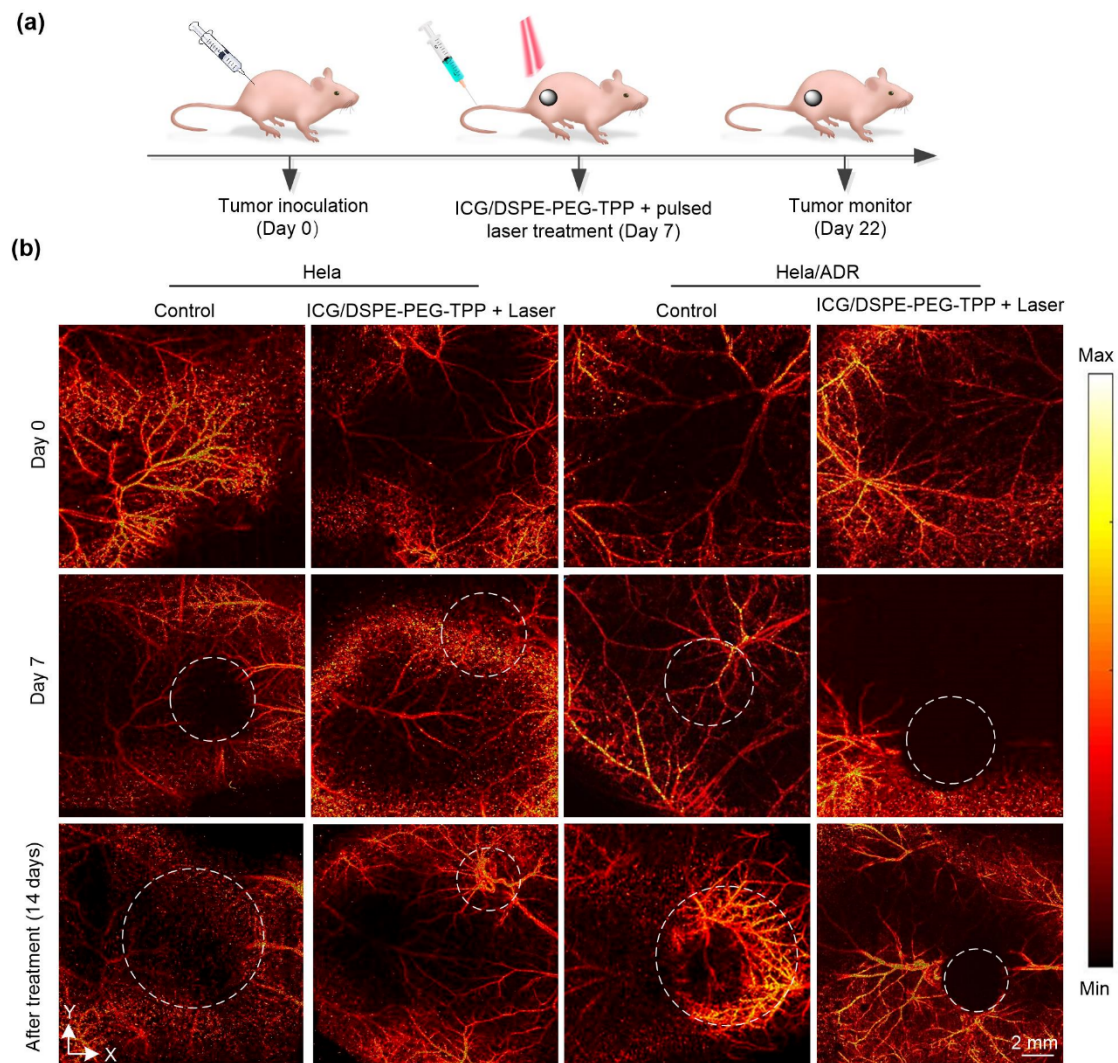


Figure S9. Photoacoustic imaging of blood vessels in tumor region. (a) Schematic diagram of monitoring tumor implantation and treatment process. (b) Representative photoacoustic vascular images of tumor bearing mice with HeLa or HeLa/ADR cells at certain time after different treatments at the tumor region.

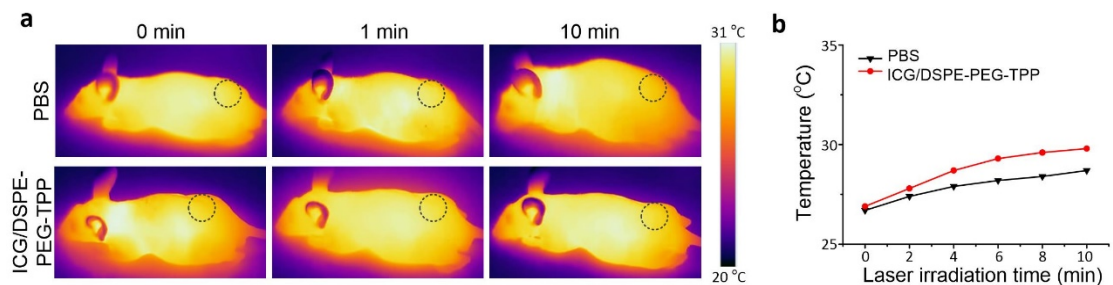


Figure S10. *In vivo* whole-body thermal images of HeLa cell bearing mice treated with PBS, ICG/DSPE-PEG-TPP (5 mg/kg, 100 μ L) after pulse laser irradiate at tumor region (780 nm, 20 mJ cm⁻²) for 10 min; images were obtained by an infrared thermometer.

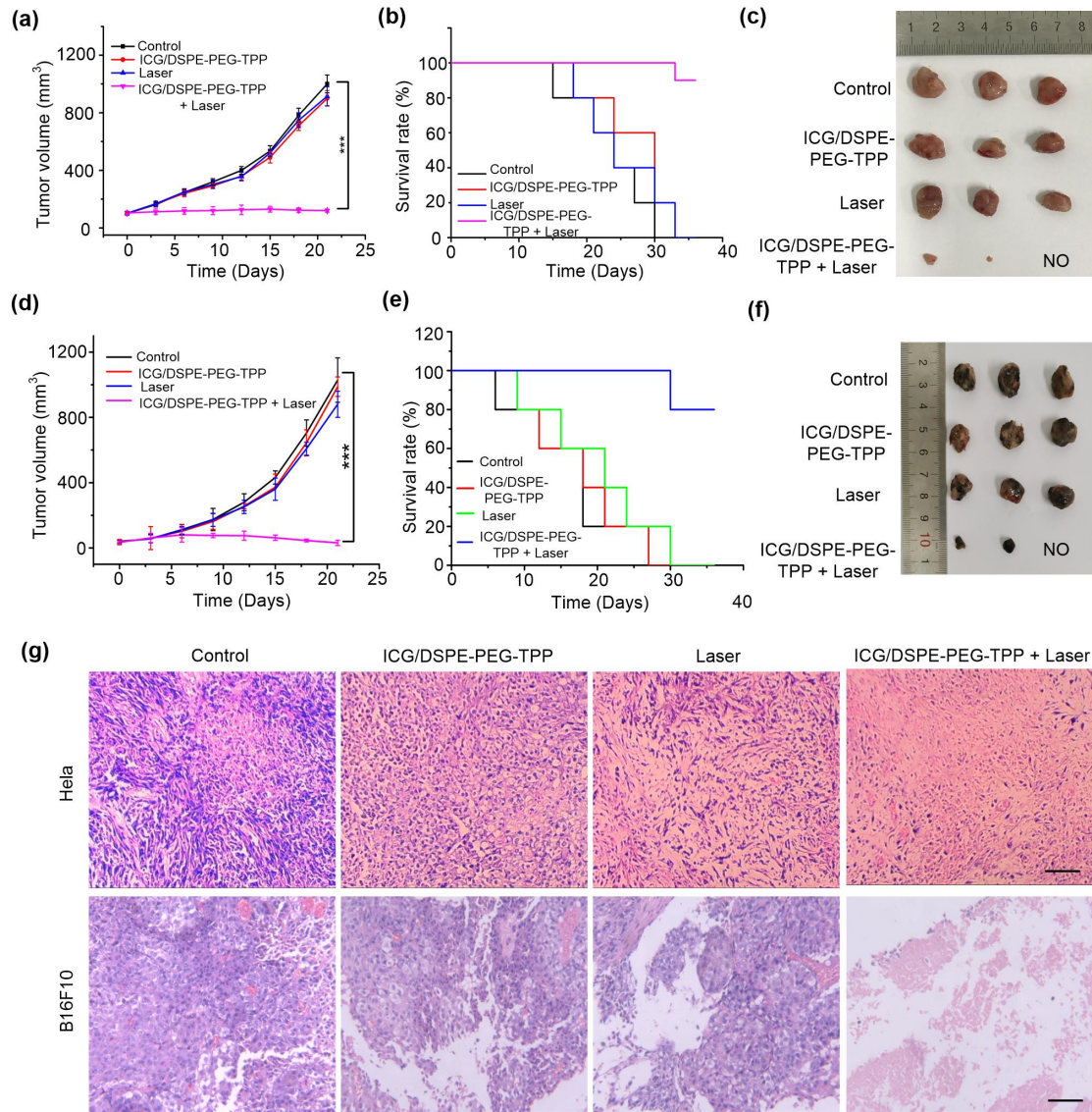


Figure S11. *In vivo* cancer inhibition evaluation in HeLa and B16F10 tumor bearing mice. (a, d) HeLa and B16F10 tumors growth curve in each treating group. (b, e) HeLa and B16F10 tumors survival curve of cancer-bearing mice after different treatments. (c, f) Typical photographs of HeLa and B16F10 tumors after different treatments collected at the 21th day. (g) H&E images of tumors after different treatments. (Scale bar: 100 μm; $n = 5$). Data are shown as mean \pm SD. * $p < 0.05$, ** $p < 0.01$, *** $p < 0.001$, compared with the control group.

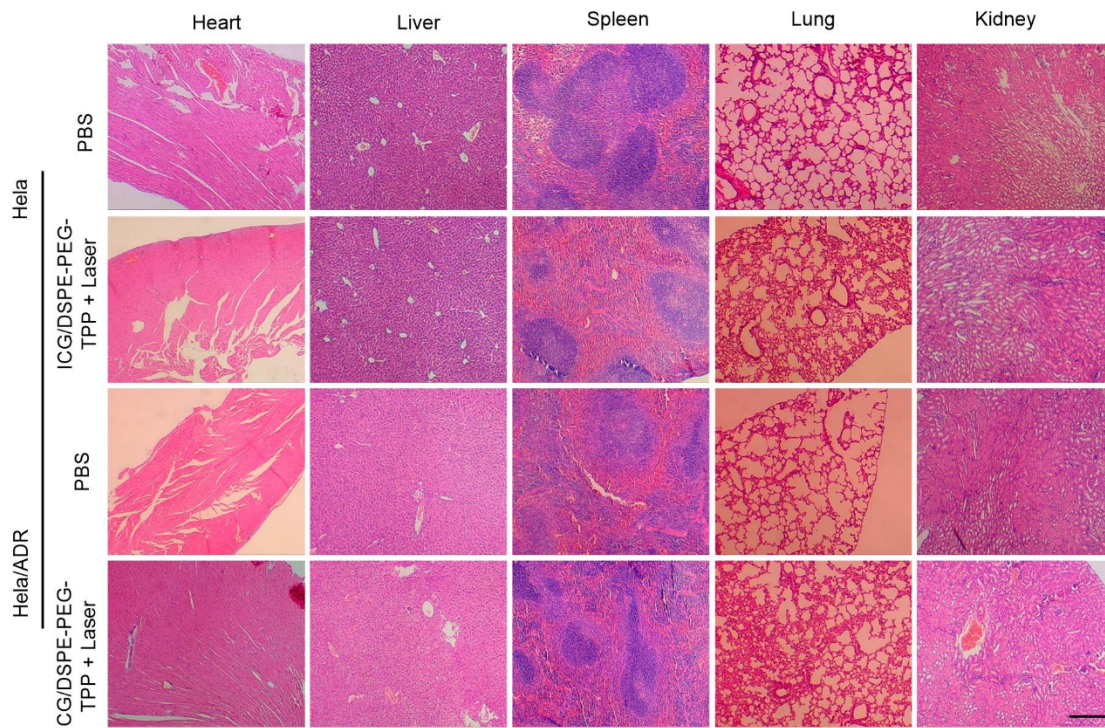


Figure S12. Safety evaluation of different treatment groups in Hela and Hela/ADR tumor bearing mice. Hematoxylin and eosin (H&E) staining of the major organs including the heart, liver, spleen, lung and kidney and observed under a microscope.

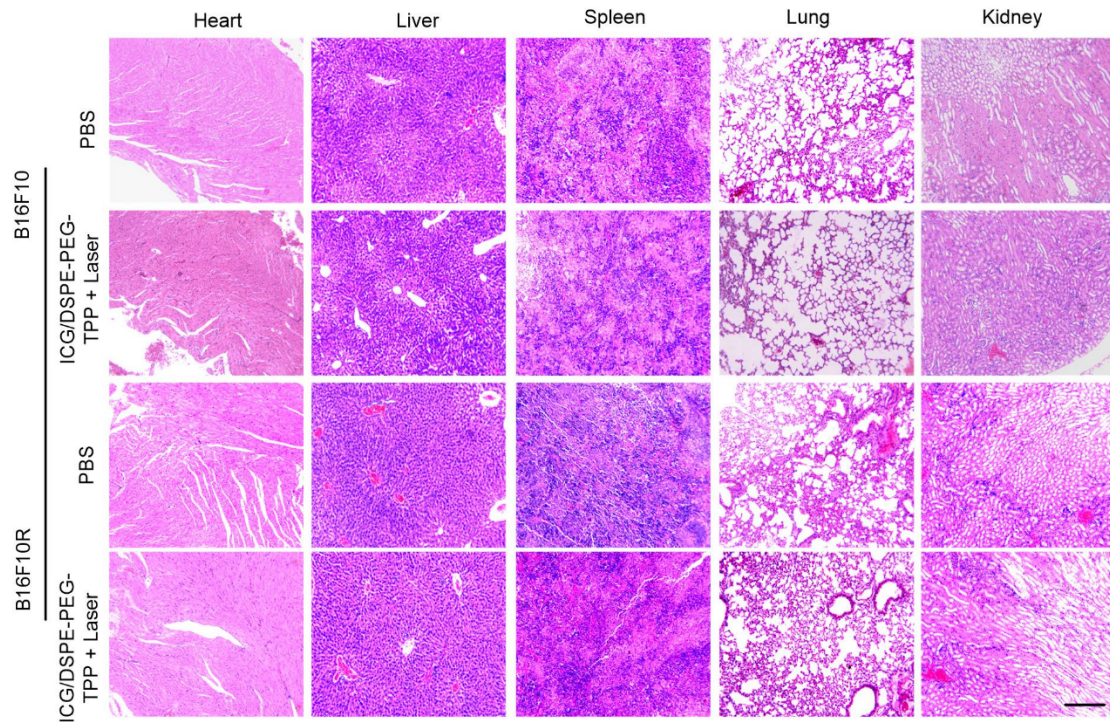


Figure S13. Safety evaluation of different treatment groups in Hela and Hela/ADR tumor bearing mice. H&E staining of the major organs including the heart, liver, spleen, lung and kidney and observed under a microscope.